


# Self-organizing hair peg-like structures from dissociated skin progenitor cells: New insights for human hair follicle organoid engineering and Turing patterning in an asymmetric morphogenetic field

Erin L. Weber<sup>1,2</sup> | Thomas E. Woolley<sup>3</sup> | Chao-Yuan Yeh<sup>1</sup> | Kuang-Ling Ou<sup>1,4,5</sup>  | Philip K. Maini<sup>6</sup> | Cheng-Ming Chuong<sup>1,7</sup>

<sup>1</sup>Department of Pathology, Keck School of Medicine of the University of Southern California, Los Angeles, California

<sup>2</sup>Division of Plastic and Reconstructive Surgery, Keck School of Medicine of the University of Southern California, Los Angeles, California

<sup>3</sup>Cardiff School of Mathematics, Cardiff University, Cardiff, UK

<sup>4</sup>Ostrow School of Dentistry of the University of Southern California, Los Angeles, California

<sup>5</sup>Division of Plastic and Reconstructive Surgery, Department of Surgery, Tri-Service General Hospital, National Defense Medical Center, Taipei, Taiwan

<sup>6</sup>Wolfson Centre for Mathematical Biology, Mathematical Institute, Oxford, UK

<sup>7</sup>Integrative Stem Cell Center, China Medical University, Taichung, Taiwan

## Correspondence

Cheng-Ming Chuong, Keck School of Medicine of the University of Southern California, Los Angeles, CA.  
Email: cmchuong@usc.edu

## Funding information

National Institute of Arthritis and Musculoskeletal and Skin Diseases, Grant/Award Number: AR 47364 and AR 60306; National Science Foundation, Grant/Award Number: DMS1440386; California Institute for Regenerative Medicine; American College of Surgeons; L. K. Whittier Foundation; A.P. Giannini Foundation

## Abstract

Human skin progenitor cells will form new hair follicles, although at a low efficiency, when injected into nude mouse skin. To better study and improve upon this regenerative process, we developed an in vitro system to analyse the morphogenetic cell behaviour in detail and modulate physical-chemical parameters to more effectively generate hair primordia. In this three-dimensional culture, dissociated human neonatal foreskin keratinocytes self-assembled into a planar epidermal layer while fetal scalp dermal cells coalesced into stripes, then large clusters, and finally small clusters resembling dermal condensations. At sites of dermal clustering, subjacent epidermal cells protruded to form hair peg-like structures, molecularly resembling hair pegs within the sequence of follicular development. The hair peg-like structures emerged in a coordinated, formative wave, moving from periphery to centre, suggesting that the droplet culture constitutes a microcosm with an asymmetric morphogenetic field. In vivo, hair follicle populations also form in a progressive wave, implying the summation of local periodic patterning events with an asymmetric global influence. To further understand this global patterning process, we developed a mathematical simulation using Turing activator-inhibitor principles in an asymmetric morphogenetic field. Together, our culture system provides a suitable platform to (a) analyse the self-assembly behaviour of hair progenitor cells into periodically arranged hair primordia and (b) identify parameters that impact the formation of hair primordia in an asymmetric morphogenetic field. This understanding will enhance our future ability to successfully engineer human hair follicle organoids.

## KEYWORDS

hair follicle, organogenesis, periodic pattern formation, skin reconstitution, tissue engineering

## 1 | INTRODUCTION

The basic tenet of plastic surgery is the restoration of form and function. However, replacing skin and functional appendages remains challenging. The hair follicle is a mini-organ, which, in association with the attached sebaceous gland, plays a crucial role in skin moisture, thermal regulation, protective sensation and aesthetic appearance. For burn patients, the loss of pilosebaceous units leads to dry, brittle skin which is more susceptible to injury. While transplantation is currently the best option for hair follicle replacement, the process requires a large number of donor follicles, which burn patients typically lack, and targets only the scalp. The ability to tissue engineer an unlimited source of pilosebaceous units for transplantation, either singly or appropriately patterned within bioengineered skin, would provide a much-needed solution for many patients.

Multiple different approaches have attempted to produce reconstituted skin with hair in mouse and humans.<sup>[1]</sup> In the mouse, we demonstrated that dissociated epidermal and dermal cells from newborn mouse skin self-assemble in vitro into multi-layered skin organoids containing placodes and dermal condensates, the two stem cell populations necessary for hair follicle development.<sup>[2,3]</sup> When grafted onto a full thickness dermal wound on a nude mouse, the cultured organoids formed mature, cycling hair follicles within a planar skin configuration. Transcriptomic analysis of the murine skin organoids has identified factors that can rescue the hair forming ability of adult mouse cells.<sup>[4]</sup> However, similar success with human cells has been more difficult. Adult human scalp cells will produce new follicles in in vivo mouse models, albeit at low rates.<sup>[5,6]</sup> The use of fetal, rather than adult, scalp enhances the efficiency of human hair follicle regeneration but a persistent lag time of 3 months to follicle formation indicates that more must be understood about follicular morphogenesis.<sup>[7,8]</sup> Despite several different approaches, efficient, large-scale, therapeutic tissue engineering and transplantation of reconstituted human skin with pilosebaceous units remains a challenge to the field.

There are two different strategies to produce hair follicles from dissociated cells. One is to use 3D printed tissue scaffolds and place cells at key positions for further morphogenesis;<sup>[9]</sup> the other is to rely on the self-organizing ability of skin progenitor cells.<sup>[4]</sup> Different progenitor cell states can be utilized for the self-organizing strategy, such as induced pluripotent cells (iPS).<sup>[10]</sup> On some occasions, cells need “help” to interact with other cells or require particular molecular signals to move forward to the next stage. Currently, in the emerging field of synthetic biology, methods are under development to provide cells with “help” in topological arrangement<sup>[11,12]</sup> or molecular signalling at the right time and place.<sup>[13]</sup>

But, to effectively adopt the synthetic biology approach, we must learn more about organoid cultures made of cells from different ages, locations or species, so we can apply key molecules to restore hair forming ability.<sup>[4]</sup> To this end, we sought to develop a three-dimensional, culture system in which different types of skin

progenitors, such as epidermal- or dermal-like somatic cells, embryonic stem cells or iPS cells, can be guided to form ectodermal organs in a planar configuration (Figure S1).<sup>[14]</sup> We hope that this culture model may serve as a platform to identify the critical factors needed, step by step, for the development of individual ectodermal organs. Here, we present our progress towards the formation of human hair follicle organoids. Within this in vitro model, we observed two distinct and novel phenomena. First, hair peg-like structures emerged after only 4 days in culture and possessed molecular and cellular characteristics similar to authentic human hair pegs. Second, the formative process of periodic patterning was quite apparent: dissociated dermal cells assembled into stripes, clusters, then distinct dermal condensations, followed by epidermal “stalks” with dermal papilla-like “caps.” The process reproducibly began at the droplet boundary and emanated as a circumferential wave towards the centre of the culture.

In vivo, periodic hair and feather placodes form in a progressive wave, propagating in different directions depending on body site (e.g. scalp and trunk). This implies that the process is a combination of local periodic patterning events and an asymmetric global influence that make the morphogenetic field asymmetric. The local periodic patterning event may involve chemical and mechanical feedback between cells and their environment.<sup>[15,16]</sup> Several models have been proposed, ranging from chemical-based reaction-diffusion models to ones where the “reactants” are cells themselves to mechanochemical models which couple cell interactions with chemical signals.<sup>[17-19]</sup> The self-organizing patterns observed experimentally in our culture system resemble patterns most simply illustrated by the Turing activator-inhibitor model.<sup>[20,21]</sup> The global behaviour of the system can be described by the occurrence of a Turing instability on an asymmetric morphogenetic field. Such asymmetry is speculated to be caused by mechanical or chemical forces or uneven cell proliferation or death.<sup>[22,23]</sup>

The droplet culture system described here provides a unique opportunity to study both periodic patterning and global events in human hair follicle formation. The formation of hair peg-like structures occurs more rapidly than other current methods and, yet, is slow enough to permit the analysis and optimization of the sequence of cellular events. Mathematical modelling of the formation wave in the hair peg population allows us to analyse the self-assembly process and predict conditions that may enhance organoid formation. Translationally, this culture system provides proof of concept that structures resembling human hair follicle precursors can be engineered in vitro in a time-efficient manner and serves as a platform to identify the optimal conditions with which to efficiently engineer human hair follicles for transplantation.

## 2 | METHODS

### 2.1 | In vitro hair follicle reconstitution assay

Epidermal and dermal cells were enzymatically and mechanically separated from neonatal foreskin and second-trimester fetal scalp

(estimated gestational age (EGA) 17-19 weeks), respectively.  $2 \times 10^6$  cultured neonatal foreskin keratinocytes and  $3 \times 10^6$  fresh fetal scalp dermal cells were resuspended in 140  $\mu$ l of F12:DMEM (1:1) medium with 5% FBS and P/S/A and plated as a droplet on a six-well cell culture insert. The droplets were incubated at 37°C and 5% CO<sub>2</sub> for 4-7 days. Growth factors were added daily. See supplemental methods for details.

## 2.2 | Patch assay

$2 \times 10^6$  neonatal foreskin keratinocytes and  $3 \times 10^6$  fetal scalp dermal cells were injected subcutaneously into the deep dermis of 6- to 12-week-old hairless nude mice. Subcutaneous nodules with formed hair follicles were harvested 8 weeks later.

## 2.3 | Immunostaining, lentiviral vectors and live cell imaging

See supplemental method, Tables S1 and S2.

## 2.4 | Mathematical modelling

A reaction-diffusion model was developed to simulate the interaction of two, as of yet, experimentally unidentified, different morphogen populations. Details, equations and parameter definitions are included in supplemental methods.

## 3 | RESULTS

### 3.1 | Human fetal scalp dermal cells induce the self-organization of hair peg-like structures in droplet culture

Dissociated neonatal human foreskin keratinocytes and 17- to 19-week EGA human fetal scalp dermal cells were mixed and co-cultured in three-dimensional droplets (Figure 1A). Within 24 hours, the epidermal and dermal cells segregated into two layers, with epidermal cells adhering to the cell culture insert membrane at the base of the droplet and dermal cells overlying the keratinocytes in a more superficial layer (Figure 1B). Around 48 hours, dermal cells began to organize, forming a trabecular mesh pattern, which then evolved into punctate cell clusters. By 72 hours, keratinocytes abutting the dermal clusters rearranged into a concentric pattern and, within 96 hours, keratinocyte "stalks" protruded, against gravity, into the droplet space, in association with a dermal cell "cap" (Figure 1B, Movie S1A-C). In comparison with 17-week EGA fetal scalp sections, the newly formed structures resemble early hair pegs, a stage in follicle development in which the invaginating keratinocytes protrude downward into the dermal plane, guided by the dermal papilla (Figure 1C). Of note, while there was a clear and early segregation of epidermal and dermal cells, we frequently encountered scattered, large, intensely keratin-positive cells interspersed within the dermal layer,

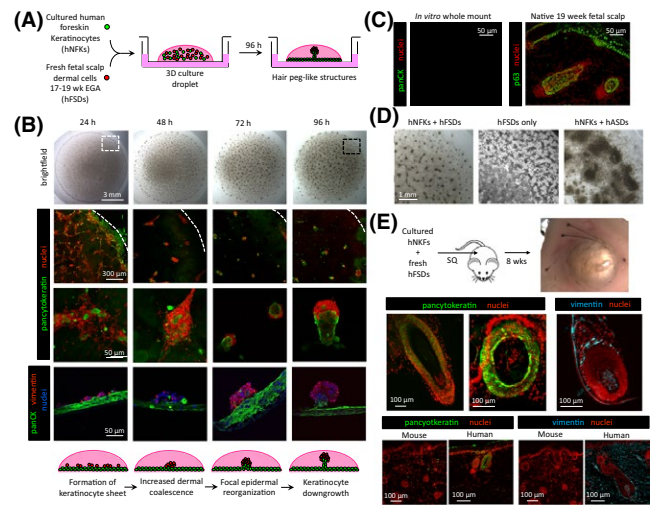


**FIGURE 1** Human neonatal foreskin keratinocytes and fetal scalp dermal cells self-organized to form hair peg-like structures in vitro. A, Schematic of the in vitro hair follicle reconstitution assay. Follicular organoids, composed of epidermal (green) and dermal cells (red), protrude from a multi-layered keratinocyte sheet (green). hNFKs = human neonatal foreskin keratinocytes, hFSDs = human fetal scalp dermal cells. B, Serial brightfield and confocal images of the culture droplet taken every 24 h demonstrated the formation of periodically arranged three-dimensional configurations by 96 h, corresponding to hair peg-like structures composed of an epidermal stalk and dermal cap. Whole mount confocal images in the second and third rows, with pancytokeratin denoting epidermal cells in green and nuclei in red, were taken from the periphery of the droplet, as represented by the white dotted box in the brightfield image in the first row. In the second row, the white dotted line demarcates the periphery of the droplet. The fourth row of images is triple-stained sections, with pancytokeratin (panCK) marking epidermal cells (green), vimentin marking dermal cells (red) and nuclei (blue) stained with TO-PRO-3 iodide. The scale bar is the same for all images per row. The large green lobules in the 48 h sample are dead cell artifacts which have trapped the fluorescent antibody ( $n = 25$ ). C, In vitro structures at 96 h (left panel) resembled hair pegs found in 19-wk human fetal scalp (right panel). p63 is a marker of epidermal progenitor cells ( $n = 25$ ). D, Human fetal scalp dermal cells alone and adult scalp dermal cells mixed with neonatal foreskin keratinocytes did not produce any hair peg-like structures after 96 h in culture. The images are taken from the periphery of the culture droplet, as exemplified by the black dotted box in B. hASDs = human adult scalp dermal cells. E, When injected subcutaneously into a nude mouse, human neonatal foreskin keratinocytes and fetal scalp dermal cells produced mature hair follicles composed of cells of human origin. Pancytokeratin (green) and vimentin (cyan) antibodies are human-specific. Sections of mouse skin were included to confirm species specificity of the antibodies (bottom panels) ( $n = 3$ )

which exhibited characteristics consistent with terminally differentiated, anucleated keratinocytes. These "cells" do not appear to participate in the morphological events.

Dermal fibroblasts are known to self-aggregate in non-adherent culture. To demonstrate that the hair peg-like structures were not an artifact of the culture system or simply a result of dermal fibroblast self-aggregation, human fetal scalp dermal cells, in the absence

of foreskin keratinocytes, were cultured under identical conditions. Fetal scalp dermal cells also formed a trabecular pattern but did not form any three-dimensional structures (Figure 1D). Similarly, adult dermal cells, from hair-bearing adult scalp, were cultured with neonatal foreskin keratinocytes. Adult scalp dermal cells formed thick, dense sheets. Neither combination produced hair peg-like structures.

### 3.2 | Hair peg-like structures in vitro displayed cytoarchitecture and molecular markers similar to those observed in vivo

Under defined conditions, epidermal and dermal cells rapidly self-assembled and transitioned through stages reminiscent of follicular development to form hair peg-like structures but failed to progress further in vitro. To verify that the human neonatal foreskin keratinocytes and human fetal scalp dermal cells possessed full regenerative potential, the same ratio of epidermal and dermal cells was injected subcutaneously into nude mice in a traditional patch assay.<sup>[2]</sup> Eight weeks later, complete hair follicles, including hair shafts, were clearly visible in the subcutaneous tissue encircling a central keratinized mass (Figure 1E). Immunostaining with human-specific antibodies confirmed that cells of the epidermal outer root sheaths and dermal papillae were of human origin (Figure 1E).

Akin to hair pegs in developing fetal skin, the reconstituted hair peg-like structures were keratin-14 positive and keratin-10 negative (Figure 2A). Keratin-10 and involucrin, markers of suprabasal cells, were expressed in all cells of the epidermal sheet except the basal layer, consistent with normal patterns of epidermal stratification (Figure 2A). While epidermal cells originally stratified with basement membrane facing the insert, the polarity of stratification was altered once epidermal downgrowth began, with epidermal “stalks” and associated dermal “caps” projecting upwards into the culture through more differentiated layers of epidermis. We suspect this is due to physical limitations of the droplet culture system. Keratinocytes of the epidermal stalk expressed K17, K18 and E-cadherin, all known to be expressed in the inner or outer root sheath layers of mature follicles, though at the hair peg stage, distinct epidermal sheath layers have not yet formed and less is known about the expected locations for expression of these proteins (Figure 2A). Some of the larger hair peg-like structures displayed longer, curving epidermal stalks, which when viewed at the right angle, appeared to possess a central keratin-positive core surrounded by concentric epidermal cells, possibly indicating progression in development towards the bulbous peg stage (Figure 2A). These advanced hair peg-like structures occurred infrequently, however, making further characterization difficult.

p63, a marker of epidermal stem cells, was initially present in all keratinocytes at 24 hours. As is seen in normal hair follicle development, p63 expression became limited to the basal layer following epidermal stratification and p63-positive cells were reproducibly noted at the leading edge of the epidermal stalk, adjacent to the dermal cap (Figure 2B). PCNA immunostaining demonstrated active cell

division in both the epidermal basal layer and the leading edge of the stalk, while the remaining epidermal cells within the stalk were quiescent (Figure 2B). The presence of focal, replicating epidermal progenitor cells at the leading edge of the stalk suggests that localized proliferation may contribute to downgrowth and we hypothesize that these proliferating cells may be putative hair matrix cells. However, we cannot rule out the possible contribution of cell migration from the adjacent stratified epidermis in hair peg formation and the mechanism by which epidermal downgrowth occurs is not yet known.

Consistent with a dermal lineage, dermal cap cells synthesized collagens I and III (Figure 2C). Basement membrane proteins, collagen IV and laminin, typically located at the interface between epidermal and mesenchymal cells within the hair follicle, were present at the junction of epidermal stalk and the dermal cap (Figure 2C, Movie S2A). Furthermore, the dermal cap cells associated with the hair peg-like structures displayed markers also present in the dermal condensate and dermal papilla. The dermal cap was composed of a heterogeneous mixture of dermal cells with a central compartmentalized area positive for alpha-smooth muscle actin ( $\alpha$ -SMA, Figure 2C, Movie S2B). While alkaline phosphatase is a classic marker of the murine dermal papilla and is expressed in the dermal papillae of 17-week human fetal scalp, there is limited and conflicting data regarding the expression of alkaline phosphatase vs  $\alpha$ -SMA in human dermal papilla cells in culture. Some publications show persistent alkaline phosphatase expression in cultured human dermal papilla cells but others demonstrate rapid loss of alkaline phosphatase expression and upregulation of  $\alpha$ -SMA expression.<sup>[24–29]</sup> In reality, the expression of dermal papilla marker genes is easily influenced by culture conditions. In our system,  $\alpha$ -SMA expression was present while alkaline phosphatase expression was not. Versican, another commonly used marker for the dermal condensate and papilla, was strongly expressed in the dermal cap (Figure 2B, C). While these dermal caps represent the developmental progression of dermal stripes to clusters to condensations and dermal papillae-like aggregates, which can functionally induce hair peg-like structures, we believe they are incomplete or immature dermal papillae because they express some, but not all, dermal papilla molecular markers and induce the formation of hair peg-like structures instead of complete hair follicles.

### 3.3 | The formation of hair peg-like structures in vitro mimics the sequential stages of development in vivo

Foreskin keratinocytes and fetal scalp dermal cells progressed through stages similar to native hair follicle development.<sup>[30]</sup> Between 48 and 72 hours in culture, epidermal cells underlying focal dermal cell collections formed a concentric pattern, distinct from the cobblestone pattern of the surrounding epidermal sheet (Figure 2D, Movie S3A,B).<sup>[31]</sup>  $\beta$ -catenin, known to be expressed in the epidermal placode and required for hair follicle morphogenesis, was focally enriched in epidermal cells abutting the clustered dermal cells, but absent from the adjacent epidermis at the time of



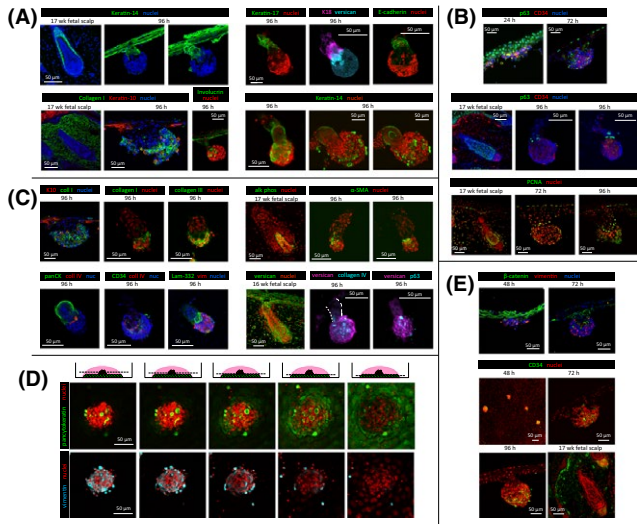


**FIGURE 2** Hair peg-like structures formed in vitro expressed appropriate epidermal and dermal markers and progressed through reproducible stages reminiscent of early hair follicle development. A, Staining of sections of hair peg-like structures with keratin-14 (green) demonstrated clear separation between epidermal and dermal cells (top left). Consistent with patterns of keratin expression in human fetal scalp, epidermal cells within the in vitro hair peg-like structures did not express keratin-10 (red). Involucrin (green), a marker of keratinocyte terminal differentiation, was highly expressed in only a portion of the epidermal sheet, which, along with keratin-10 expression, suggests stratification (bottom left). Involucrin also strongly marked cells believed to be terminally differentiated, anuclear corneocytes that became inappropriately trapped within the dermal cell cap. The epidermal stalks were keratin-17 (green), keratin-18 (magenta) and E-cadherin (green) positive (whole mount, top right). Several of the larger hair peg-like structures appeared to have epidermal stalks with central lumens and concentrically organized keratinocytes, marked by keratin 14 (green) (whole mount, bottom right). B, At 24 h, all keratinocytes expressed p63 (green), a marker of epidermal stemness (sections, top panel). By 72 and 96 h, p63-positive cells were localized to the basal layer of the epidermal sheet and the leading edge of the epidermal stalk abutting the dermal cap (middle panel). 96-h images are whole mount specimens. PCNA-positive (green), actively proliferating cells were present within the basal layer of the epidermal sheet, the epidermal stalk at the interface with the dermal cap and the periphery of the dermal cap, similar to 17-wk second-trimester human fetal scalp (sections, bottom panel). C, The cells of the dermal cap expressed collagen I (green, section and whole mount) and collagen III (green, whole mount) (top left). K10 = keratin-10. Collagen IV (red) and laminin-332 (green), markers of the dermal papilla basement membrane, were expressed at the interface between epidermal and dermal cells within the hair peg-like structures in vitro (whole mount, bottom left). PanCK = pancytokeratin, nuc = nuclei, vim = vimentin.  $\alpha$ -SMA (green), a marker of human dermal papilla cells in culture, was expressed within the centre of the dermal cap (whole mount, top right). Human dermal papilla cells in vivo express alkaline phosphatase (alk phos (green), left image), a marker which is typically lost during in vitro culture. The dermal cap was also positive for versican, a commonly used dermal condensate or dermal papilla marker (whole mount, bottom right). D, Serial optical sections of a dermal aggregate at 48 h imaged at increasing droplet depths demonstrated a rounded, dense dermal cluster atop an epidermal sheet with concentrically arranged nuclei, reminiscent of the epidermal placode. E,  $\beta$ -catenin was expressed throughout the epidermal sheet at 48 h but was restricted to those epidermal cells associated with the dermal cap by 72 h (sections, top panels). Dermal cells within the dermal cap were positive for CD34, a marker of the early dermal papilla stem cell (bottom panels). The 48-h image is a whole mount specimen. All other images are sections. All staining was performed on multiple hair peg-like structures from at least three biological replicates ( $n = 3$ )

epidermal downgrowth (Figure 2E).<sup>[32–34]</sup> Cells within the dermal clusters expressed CD34, a marker of the human dermal condensate and early dermal papilla (Figure 2E).<sup>[35]</sup> The formation of hair germ-like structures and, then, hair peg-like structures ensued between 72 and 96 hours in culture.

Live cell confocal imaging of the droplet culture was developed to visualize the cell-cell interactions and collective cell movements during hair peg formation. Visual discrimination between epidermal and dermal cells was achieved using epidermal-specific promoters. Lentiviral transduction to express lineage-specific fluorescent markers did not perturb hair peg development in vitro (Figure S2). A view from the top of a two-colour, live cell culture droplet demonstrated distinct spherical dermal caps are shown in the Supplement Material (Figure S2, Movie S4). Nuclei of cells at the periphery of the dermal cap exhibited a curved morphology, and cells near the centre of the dermal cap displayed increased local cell motion while cells at the periphery were more stationary, suggesting a heterogeneity of dermal cell function. In contrast, cells within the epidermal sheet remained static. Three-colour live imaging distinguished K14+ epidermal cells (yellow), p63+ epidermal precursor cells (magenta) and dermal cells (cyan) within the hair peg and adjacent epidermal sheet (Figure S2, Movie S5A, B). As seen in static confocal images, p63-positive cells were noted within the epidermal sheet as well as the epidermal stalk of the hair peg. Several strongly positive p63 cells were present at the leading edge of the epidermal stalk, abutting the dermal cluster, and 1–2 cells were consistently noted at the opposite pole of the dermal cluster, a unique position which could suggest an instructive role in directional epidermal downgrowth.

### 3.4 | Hair peg-like structure formation in the organoid droplet culture displays spatiotemporal patterning

Large-scale dermal cell patterns within the droplet culture demonstrated a spatiotemporal progression, which initiated at the

droplet periphery and advanced towards the centre (Figure 3A). At 24 hours postplating, dissociated dermal cells remained distributed in a homogeneous layer without a distinct macroscopic pattern. Over the next 12 hours, dermal cells coalesced into long undulating stripes of higher dermal cell density. By 48 hours in culture, long stripes had subdivided into shorter stripes and, over

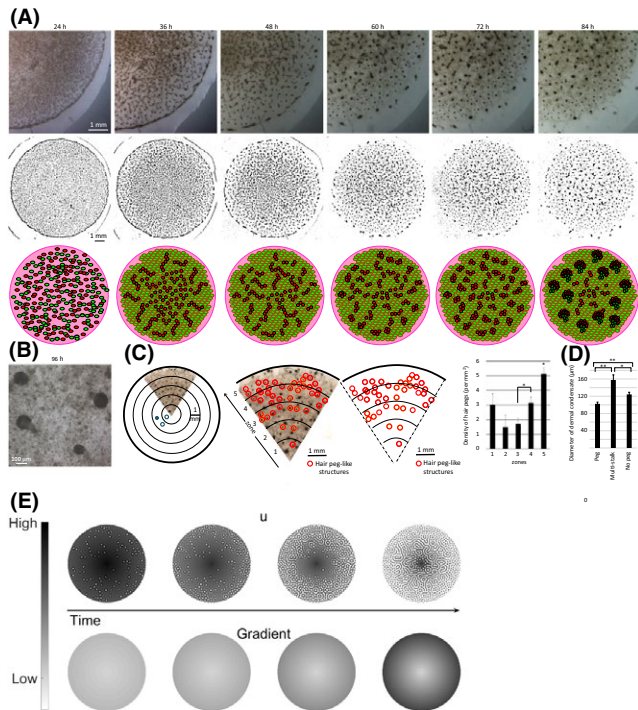


**FIGURE 3** Collectively, a stripe-to-dot formative gradient forms from the centre to periphery of the culture droplet and suggests a Turing periodic patterning process on an asymmetric field. A, Brightfield images of a single culture droplet taken every 12 h demonstrated the formation of an initial trabecular pattern, which then gave way to the periodically arranged stripes and cell clusters (top row). Line drawings created from brightfield images (middle row) and a schematic where red represents dermal cells and green represents epidermal cells (bottom row) emphasize the transitions in distinct periodic patterns as they relate to developmental stages ( $n = 4$ ). B, High-power magnification demonstrates the hair peg-like architecture under brightfield imaging ( $n = 4$ ). C, The field was divided into five concentric zones. Anatomic hair peg-like structures developed at a higher density in zones 4-5, towards the periphery of the droplet. In paired  $t$  test comparisons, the average density of hair peg-like structures at the periphery of the culture droplet was statistically different from more central zones ( $*P < 0.05$ ). Error bars represent standard error of the mean ( $n = 11$ ). D, Dermal clusters of a smaller diameter were more likely to be associated with single stalked hair peg-like structures than were larger dermal clusters found at the centre of the droplet. Average cluster diameter is plotted. Paired  $t$  test comparisons were used to examine statistically significant differences between groups. Error bars represent standard error of the mean.  $*P < 0.05$ ,  $**P < 0.01$  ( $n = 3$ ). E, Numerical simulations of reaction-diffusion equations are presented in the methods section. The top row illustrates how the density of activator ( $u$ ) alters over time, with darker colours presenting high-density regions and lighter colours representing low-density regions. The bottom row illustrates the radially symmetric spatiotemporal gradient field that alters the properties of the reaction-diffusion equations heterogeneously across the domain. As time increases, the value of the field at the boundary increases to a maximum value and the gradient gets steeper. We see that as the gradient steepens, the activator pattern transitions from spots at the periphery to labyrinthine patterns in the centre, which recapitulates the *in vitro* periodic patterns. Additional parameter values are given in Table S3

time, short stripes became rounded, CD34-positive dermal clusters (Figure 2F). Between 72 and 96 hours, hair peg-like structures formed (Figure 3B), first at the droplet periphery. In addition to forming earliest, elongated structures approximating more mature hair peg-like structures formed more densely at the periphery (Figure 3C, D). Centrally, dermal aggregates were 60% larger in diameter, which correlated with the formation of less mature hair peg-like structures and, in many cases, abnormal aggregates possessing multiple epidermal stalks (Figure 3D). The formative wave of “long stripe—short stripe—rounded cluster—peg-like structure” advanced from the periphery towards the centre of the droplet, with each new change in morphology, and the stripe and spot patterns are reminiscent of the periodic patterns predicted by Turing activator-inhibitor principles.<sup>[36,37]</sup>

### 3.5 | Mathematical modelling simulates the observed spatiotemporal patterns

Reaction-diffusion systems are capable of spontaneously producing sustained spatial patterns. Specifically, spots, stripes and labyrinthine patterns are all possible within the framework of diffusion-driven instability, known as Turing patterns. Once formed, generally only one of these patterns is selected and remains fixed.<sup>[38]</sup> In contrast, in our droplet culture, multiple distinct patterns occur simultaneously and are formed in serial progression at different locations within the droplet. As mentioned, such patterning complexity can arise from several different sources. We chose to use a reaction-diffusion description because the transition between spots and stripes is well understood.<sup>[38,39]</sup> Critically, in two dimensions, Turing patterns can produce spots and/or stripes, but typically not at the same time.<sup>[21]</sup> It is simply the competition between the quadratic and cubic terms of the activator kinetics that determine which pattern mode is obtained.<sup>[21]</sup> Thus, if the correct pattern kinetics are chosen to produce in phase, or out of phase, concentration patterns, then any Turing system can be guided to give rise to spots and/or stripes. Further, a parameter's influence is extremely local in Turing patterns.<sup>[22]</sup> Thus, all we require to convert a system from spots to stripes is to use a gradient that influences the competition between the cubic and quadratic term. Hence, this is a completely general and robust mechanism for producing such dynamics. Based on this, we propose that an asymmetric spatiotemporal gradient is present to explain the mixed spectrum of patterns within the space (organoid droplet) and the transition of patterns over time. The work implies that the droplet represents an asymmetric morphogenetic field. Indeed, in embryonic development, hairs and feathers form in propagative waves in different body domains, rather than simultaneously.<sup>[40-42]</sup> This gave us the motivation to develop a simulation of Turing patterning occurring in an asymmetric morphogenetic field (Figure 3E).

To make the simulation model more broadly applicable, we purposely assigned the morphogens generic activator or inhibitor functions, rather than focusing on specific signalling molecules (please refer to the supplemental methods for a more detailed description). Critically, this work is not about specifying the exact underlying

kinetics. Indeed, we do not have sufficiently detailed information to determine the system to this accuracy. The specific use of our model is to highlight that the transition seen in the experiments can be captured, quite generally, using a simple radially symmetric, linear, time-dependent gradient. The observed result could be obtained in an infinite number of more complicated ways. However, our results have put a lower bound limit on the complexity required to make a model consistent with the observed results.

Since we observe that hair peg-like structures first form in the periphery, the asymmetry suggests that the activator becomes increasingly sensitive to the inhibitor morphogen  $v$ , at the periphery, or, alternatively, the activator becomes decreasingly sensitive to the activator's self-activation response. Such a gradient can easily arise as the experimental droplet is anisotropic, and could be due to chemical signalling (e.g. growth factors) or physical forces in nature, or both. Thus, the principles of Turing activator and inhibitor remain the same, but in different regions, we anticipate the field can be heterogeneously predisposed with parameters that favour or suppress periodic patterning. As time progresses, the gradient increases towards the periphery (bottom simulations of figure "simulation"), and patterns transit from labyrinthine stripes to spots (top simulations of figure "simulation") (Figure 3E). The spatiotemporal heterogeneity is modelled as a linear spatial gradient that increases at the droplet boundary and fixes over time (Figure 3E, Movie S6). The visualization of the gradient exhibits itself as a hair peg formative wave travelling from the periphery towards the centre of the field, matching experimental results observed in the droplet cultures. Critically, the proposed asymmetry could be wrapped up inside the equations, but this would obscure the essential requirement of a spatiotemporal gradient appearing. Thus, we choose to be explicit with the addition of such complexity.

### 3.6 | A platform to modulate hair peg morphogenesis in vitro

To increase the number of hair peg-like structures and to stimulate development beyond the hair peg stage, we modulated multiple parameters within the droplet culture system. The greatest number of hair peg-like structures per droplet culture was generated with a 150  $\mu$ L volume droplet, 5% FBS concentration and epidermal to dermal cell ratio of 2:3 (Figure 4A). An average of 286 hair peg-like structures ( $\pm 138$ ) per  $\text{cm}^2$  with an interfollicular distance of 350  $\mu$ m was produced under optimal conditions (Figure 4B). For comparison, endogenous hair pegs from 17-week fetal scalp are spaced, on average, 235  $\mu$ m apart. The in vitro hair peg-like structures were similar in overall shape to hair pegs of 17-week fetal scalp but exhibited significantly different structural proportions. The reconstituted hair peg-like structures possessed shorter, narrower keratinocyte stalks and wider dermal caps while the height of the dermal cap remained consistent with endogenous fetal hair pegs (Figure 4B). Native fetal scalp exhibited hair pegs of various epidermal stalk heights. The reconstituted hair peg-like structures were, on average, shorter than the endogenous hair pegs but more closely resembled the shorter,

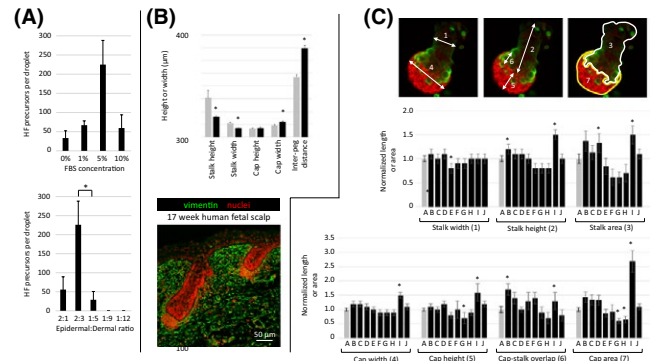


**FIGURE 4** Modulation of hair peg morphogenesis in vitro. A, Here, we examine the conditions that can influence the number, size and progression of the hair peg-like structures. Hair peg-like structures formed more frequently when culture medium contained 5% FBS and when an epidermal to dermal cell ratio of 2:3 was used. The average number of hair peg-like structures formed per condition is plotted, with error bars representing standard error of the mean and statistical significance assessed with paired  $t$  tests.  $*P < 0.05$  ( $n = 6$ ). B, The in vitro hair peg-like structures (black bars) show similar architecture to hair pegs in 17-wk human fetal scalp (grey bars). However, the average stalk height, stalk width and cap width of the in vitro hair peg-like structures were significantly smaller. While the in vitro hair peg-like structures formed at regular intervals, there was a larger average interfollicular distance than is found in fetal scalp tissue. An asterisk denotes a  $P$ -value of  $< 0.05$ , when compared to native human fetal scalp, via paired  $t$  tests. Error bars represent standard error of the mean ( $n = 5$ ). C, The addition of growth factors to the droplet cultures caused significant changes in certain aspects of the epidermal stalk and dermal cap dimensions, but did not induce further development into a bulbous peg structure. Dimensions measured the following: 1) epidermal stalk width, 2) epidermal stalk length, 3) epidermal stalk area at the structure midpoint, 4) dermal cap width, 5) dermal cap height, 6) epidermal stalk-dermal cap overlap and 7) dermal cap area at the structure midpoint. Growth factors: A) negative control, B) Shh 1  $\mu\text{g/mL}$ , C) Tgfb2 0.5  $\mu\text{g/mL}$ , D) RAR antagonist ER50891 1  $\mu\text{mol/L}$ , E) FGF7+ FGF10 1  $\mu\text{g/mL}$ , F) FGF2 1  $\mu\text{g/mL}$ , G) FGF2+ Shh 1  $\mu\text{g/mL}$ , H) FGF2+ Wnt7a 1  $\mu\text{g/mL}$ , I) PKCi 660 nmol/L chelerythrine chloride and 10 nmol/L bisindolylmaleimide I and J) Noggin 1  $\mu\text{g/mL}$ . All measurements were normalized to the negative control, and average dimensions are shown. Error bars represent standard error of the mean. Statistical significance between two groups was calculated using paired  $t$  tests. An asterisk denotes a  $P$ -value  $< 0.05$ , compared to the negative control without added factors ( $n \geq 3$ )

early hair pegs in native skin, suggesting that, according to normal developmental patterns, the reconstituted hair peg-like structures could be expected to elongate further before transitioning to the bulbous peg stage. However, our reconstituted hair peg-like structures failed to progress further when they were maintained for three additional days in culture. Clearly, other factors are required.

Although we have not been able to achieve more mature hair follicle formation, the self-organization of periodically arranged hair peg-like structures from dissociated cells is a remarkable process. Detailed analysis of the process enables this droplet culture to serve as a platform for large-scale screening of experimental conditions

to optimize in vitro follicle formation. We identified four possible signals that might support developmental progression: (a) increased dermal signalling for epidermal downgrowth (Shh, Tgf $\beta$ 2), (b) stronger dermal papilla inductivity (Wnt7a, FGF2), (c) inhibition of premature keratinocyte differentiation (protein kinase C (PKC), Noggin, retinoic acid receptors (RAR)) and (d) stimulation of keratinocyte differentiation and/or stratification (FGF2, FGF7/10).<sup>[43–50]</sup>

Exogenous growth factors were added to the culture medium every 24 hours. A range of concentrations was tested for each protein; results for the concentration which produced the greatest effect are shown (Figure 4C). Thus far, none of the added factors have resulted in progression to the next stage, the bulbous hair peg. However, a detailed analysis of dermal cap and epidermal stalk width, height and area identified significant changes mediated by the added growth factors, which, with more investigation, may hold the key to stimulating true follicle formation in culture. Cap and stalk sagittal areas maintained a linear relationship with the total cap and stalk volumes, emphasizing the radial symmetry of these structures and allowing us to simplify analysis by measuring the area of each structure at the midpoint corresponding to maximal width (Figure S3). During the early peg to bulbous peg transition, the dermal cap becomes more compact and is encapsulated by the base of the elongating epidermal sheath.<sup>[30]</sup> The addition of 1  $\mu$ mol/L Shh stimulated epidermal downgrowth, resulting in longer epidermal stalks, as well as a change in the dermal cap shape, with an increased width and cap-stalk overlap, suggesting that Shh may stimulate dermal cell migration proximally along the epidermal stalk or, conversely, epidermal stalk displacement of dermal cap cells (Figure 4C). The protein kinase C inhibitors, chelerythrine chloride and bisindolylmaleimide I, produced a similar effect, with increased epidermal stalk length and overall stalk area, as well as increased dermal cap area and cap-stalk overlap. FGF2, in combination with Shh, decreased dermal cap height and area and the retinoic acid receptor antagonist ER50891 enhanced total stalk area. Though subtle changes were evident when exogenous factors were added, they were insufficient to alter the gross morphology of the hair peg-like structure and push development into the bulbous peg stage.

## 4 | DISCUSSION

The ability to tissue engineer human hair follicles for transplantation would eliminate a treatment gap for numerous patients. Over the years, our group's research has focused on the morphogenesis of skin appendages. Recently, we examined the self-organizing behaviour of dissociated epidermal and dermal newborn mouse cells and their ability to reconstitute functional follicles.<sup>[4]</sup> Similar studies of human follicular morphogenesis have been difficult to achieve, due to the low efficiency of follicle formation from readily available adult cells and the long time to follicle formation. Here, we demonstrated the production of human hair peg-like structures in vitro from a well-defined mixture of progenitor cells. In this three-dimensional organoid droplet culture, dissociated neonatal epidermal and fetal dermal

cells progressed, via self-organization, through the following reproducible and recognizable stages akin to early follicle development to reach cellular configurations similar to hair pegs in situ: (a) mixed dissociated cells, (b) cell sheets, (c) dermal stripes and clusters, (d) dermal clusters with associated epidermal placode-like collections and (e) distinct hair peg-like structures with spatial periodicity.<sup>[30]</sup> The developmental process proceeded rapidly within 96 hours and was dependent on epidermal:dermal cell ratio and factor concentration, suggesting the need for an appropriate balance of epithelial-mesenchymal signalling factors or cell-cell interactions. This in vitro culture system demonstrates the initiation and rapid progression of early stages of human follicle-like development. It also shows that human and mouse cells utilize different morphogenetic paths in the morphospace of epidermal-dermal multicellular configurations and may explain why it has been difficult to achieve robust human hair reconstitution. We hypothesize that the differences between human and mouse hair follicle reconstitution may be due to three factors: *epidermal cell plasticity, the inducing ability of dermal cells and morphogenetic field competence.*

1. *The plasticity of foreskin keratinocytes* is known to wane with prolonged culture, resulting in reduced hair follicle formation.<sup>[51]</sup> We hypothesized that a loss of epidermal plasticity inhibited further follicle organoid development in vitro beyond the peg stage. Protein kinase C (PKC) and retinoic acid pathways play a role in epidermal differentiation and stratification during skin development. Excessive retinoic acid causes cessation of hair follicle development at the germ stage in mice, while inhibition of PKC promotes folliculogenesis from adult mouse cells.<sup>[4,47,49]</sup> The addition of PKC inhibitors and an RAR antagonist exhibited positive effects on the length and diameter of the epidermal stalk but was insufficient to drive further folliculogenesis, suggesting that other factors are required for progressive development. We suspect that the less primitive epigenetic state of the keratinocytes used may be the molecular basis for suboptimal competence. In future studies, we will search for factors that can "reprogram" these keratinocytes or use more responsive keratinocytes.
2. *The inducing ability of dermal cells* is a second critical component for folliculogenesis. The dermal papilla releases multiple factors, which participate in epidermal-mesenchymal signalling during folliculogenesis. Shh and Tgf $\beta$  are necessary for epidermal downgrowth and mice which lack Shh signalling possess hair follicles which are stalled at the germ/peg stage.<sup>[43,44]</sup> The addition of Shh to the droplet cultures stimulated additional epidermal downgrowth but did not cause structural progression to the bulbous peg stage. We also examined Wnt7a and FGF2, which have been shown to maintain proliferation and inductivity in cultured murine dermal papilla cells.<sup>[45,46]</sup> Yet, we did not observe significant progress in organoid development. The dermal papilla-like cells in our culture do not appear fully functional as they can only support the induction of hair peg-like structures, not mature follicles. However, this system provides a promising platform for the



continued search for factors or conditions which enhance inductivity.

3. *The morphogenetic field*, comprised of epidermal cells, dermal cells and extracellular matrix together, must enter a competent stage for periodic patterning to begin. The developing embryo is a heterogeneous morphogenetic field with anisotropic growth in which chemical factors, cell types and mechanical forces are unevenly distributed in three spatial dimensions and one temporal dimension. Here, our organoid culture demonstrates obvious asymmetry within the droplet, as patterns began at the periphery and migrated centrally. Labyrinthine stripes of dermal cells were noted initially, which subsequently transformed into periodically arranged dermal cell clusters. Both stripes and dermal clusters can be produced by a simple Turing model and can reflect an intermediate stage of the final periodic patterns if there is an uneven morphogenetic field.<sup>[38]</sup> What can account for the difference in progression through the periodic patterning process? While a simple generic radial gradient effected by one component may be sufficient for a Turing activator-inhibitor system to produce the pattern here, it may not be sufficient to produce the complex spatiotemporal patterning transitions we observed experimentally.<sup>[36,37]</sup> Here, we purposely designed a generic model, to have wider conceptual application. Simulation with mathematical modelling suggests similar patterning sequences can be achieved through uneven chemical signalling activities<sup>[52]</sup> (e.g. higher concentration of activator morphogens at the droplet periphery or higher sensitivity of cells at the droplet periphery) or uneven mechanical forces<sup>[53]</sup> (e.g. cellular tension or matrix rigidity favour periodic formation at the droplet periphery). The mathematical and experimental models presented here will help us identify the molecular basis of these patterning processes in the analysable droplet in vitro and in the complex developing embryo in vivo in the future.

In vivo, chicken feather buds form exquisite hexagonal patterns progressively from the midline to the flank. Earlier works have suggested this results from a local Turing event and a global propagating event.<sup>[54]</sup> However, the nature of the global event was unknown. This is part of the motivation for this study, to use the organoid droplet to understand more about the nature of the sequential appearance of hair or feather primordia. It is timely that a paper reporting a global Eda wave spreading from the midline to the flank is just reported, which suggests Eda induces FGF20, followed by dermal cell aggregate formation, thus facilitating Turing patterning via mechano-chemical coupling.<sup>[55]</sup> Based on this and other studies, we propose a new understanding on the process of propagative formation of feather arrays in vivo: a local Turing periodic patterning occurs and works together with a global propagation mechanism.<sup>[56]</sup> In this new study, progressive expression of Eda and activation of Eda signalling from the midline to the flank is shown to mediate the global process by lowering the threshold of dermal condensation.<sup>[55]</sup> Yet, what is upstream to Eda remains unclear. Thus, the global mechanism can be chemical or mechanical in nature, as long as it can tilt the Turing activator/inhibitor system ratio.<sup>[56]</sup> The asymmetric

morphogenetic field in the organoid culture studied here presents a good model to further investigate how this global asymmetry mechanism works.

With two cellular components, the initial epidermal and dermal cell ratio will influence the final stable position in the morpho-space of two-component multi-cellular assemblies.<sup>[4]</sup> The initial conditions, determined by the probability of cell collision and the relative strength of cell adhesion, control the initial multi-cellular configuration. In the human cell culture droplet, epidermal-matrix adhesions appear to dominate, leading to the formation of the epidermal layer first. Dermal-dermal interactions are stronger than epidermal-dermal adhesions, leading to the formation of dermal stripes and dermal clusters. However, during morphogenetic processes, there can be “qualitative changes” of cellular collectives. Following the formation of dermal condensations, epidermal-dermal condensate adhesion increases and can induce the formation of hair peg-like structures, up to the extent that epidermal basement membrane polarity is reversed. Thus, the high-resolution analysis of the process of hair peg formation provides an excellent opportunity to fine-tune key cellular events.

In summary, we have demonstrated that human fetal scalp dermal cells, in association with competent epidermal cells, can direct the rapid regeneration of human hair peg-like organoids in vitro. The opportunity to study the asymmetric spatiotemporal sequence of periodic patterning within the droplet provides insights into the self-organizing behaviour of skin progenitor cells. Furthermore, this in vitro culture system provides an opportunity to study ways to restore and optimize hair follicle regeneration from easily obtainable adult dermal cells and may support the production of complete hair follicles for transplantation in the future.<sup>[57]</sup>

## ACKNOWLEDGEMENTS

This work was supported by funding from the American College of Surgeons (E.L.W.), the California Institute for Regenerative Medicine (E.L.W.), the A. P. Giannini Foundation (E.L.W.), a graduate fellowship from the Ministry of National Defense of Taiwan (K.L.O.), the L. K. Whittier Foundation (C.M.C.), the National Institute of Arthritis and Musculoskeletal and Skin Diseases of the National Institutes of Health (AR 47364, AR 60306; and GM125322 to C.M.C.) and the National Science Foundation (DMS1440386 to T.E.W. and P.K.M.). We thank Dr. Chin Lin Guo for helpful discussion and acknowledge the USC Research Center for Liver Disease Cell and Tissue Imaging Core and the USC Stem Cell Microscopy Core Facility for their assistance and participation. We thank Dr. R.B. Widelitz for helpful input. T.E.W. and P.K.M. thank the Mathematical Biosciences Institute (MBI) at Ohio State University for helping to initiate this research. MBI receives its funding through the National Science Foundation grant DMS1440386.

## CONFLICT OF INTEREST

The authors have declared no conflict of interest.

## AUTHOR CONTRIBUTIONS

E.L.W. and C.M.C. conceived the idea and experimental design. E.L.W. and K.L.O. conducted the experiments. C.Y.Y. provided imaging expertise. T.E.W. and P.K.M. produced mathematical modelling. E.L.W., T.E.W. and C.M.C. prepared the manuscript.

## ORCID

Kuang-Ling Ou  <https://orcid.org/0000-0001-9536-2677>

## REFERENCES

- [1] M. Takeo, T. Tsuji, *Curr. Opin. Genet. Dev.* **2018**, *52*, 42.
- [2] Y. Zheng, X. Du, W. Wang, M. Boucher, S. Parimoo, K. Stenn, *J. Invest. Dermatol.* **2005**, *124*, 867.
- [3] L. F. Lee, T. X. Jiang, W. Garner, C. M. Chuong, *Tissue Eng Part C. Methods* **2011**, *17*, 391.
- [4] M. Lei, L. J. Schumacher, Y. C. Lai, W. T. Juan, C. Y. Yeh, P. Wu, T. X. Jiang, R. E. Baker, R. B. Wideltz, L. Yang, C. M. Chuong, *Proc. Natl Acad. Sci. USA* **2017**, *114*, E7101.
- [5] C. A. Higgins, J. C. Chen, J. E. Cerise, C. A. Jahoda, A. M. Christiano, *Proc. Natl Acad. Sci. USA* **2013**, *110*, 19679.
- [6] R. L. Thangapazham, P. Klover, J. A. Wang, Y. Zheng, A. Devine, S. Li, L. Sperling, G. Cotsarelis, T. N. Darling, *J. Invest. Dermatol.* **2014**, *134*, 538.
- [7] X. Wu, L. Scott Jr, K. Washenik, K. Stenn, *Tissue Eng. Part A* **2014**, *20*, 3314.
- [8] Q. Zhang, T. Zu, Q. Zhou, J. Wen, X. Leng, X. Wu, *Regen. Med.* **2017**, *12*, 503.
- [9] H. E. Abaci, A. Coffman, Y. Doucet, J. Chen, J. Jackow, E. Wang, Z. Guo, J. U. Shin, C. A. Jahoda, A. M. Christiano, *Nat. Commun.* **2018**, *9*, 5301.
- [10] J. Lee, R. Bscke, P. C. Tang, B. H. Hartman, S. Heller, K. R. Koehler, *Cell Rep.* **2018**, *22*, 242.
- [11] K. E. Toyoshima, K. Asakawa, N. Ishibashi, H. Toki, M. Ogawa, T. Hasegawa, T. Irie, T. Tachikawa, A. Sato, A. Takeda, T. Tsuji, *Nat. Commun.* **2012**, *3*, 784.
- [12] R. Takagi, J. Ishimaru, A. Sugawara, K. E. Toyoshima, K. Ishida, M. Ogawa, K. Sakakibara, K. Asakawa, A. Kashiwakura, M. Oshima, R. Minamide, A. Sato, T. Yoshitake, A. Takeda, H. Egusa, T. Tsuji, *Sci. Adv.* **2016**, *2*, e1500887.
- [13] J. J. Velazquez, E. Su, P. Cahan, M. R. Ebrahimkhani, *Trends Biotechnol.* **2018**, *36*, 415.
- [14] S. C. Chueh, S. J. Lin, C. C. Chen, M. Lei, L. M. Wang, R. Wideltz, M. W. Hughes, T. X. Jiang, C. M. Chuong, *Expert Opin. Biol. Ther.* **2013**, *13*, 377.
- [15] P. K. Maini, R. E. Baker, C. M. Chuong, *Science* **2006**, *314*, 1397.
- [16] R. Sennett, M. Rendl, *Semin. Cell Dev. Biol.* **2012**, *23*, 917.
- [17] S. Kondo, T. Miura, *Science* **2010**, *329*, 1616.
- [18] A. Nakamasu, G. Takahashi, A. Kanbe, S. Kondo, *Proc. Natl Acad. Sci. USA* **2009**, *106*, 8429.
- [19] J. D. Murray, P. K. Maini, R. T. Tranquillo, *Phys. Rep.* **1988**, *171*, 59.
- [20] A. M. Turing, *Philos. Trans. R. Soc. Lond. B Biol. Sci.* **1952**, *237*, 37.
- [21] H. Meinhardt, *Interface Focus* **2012**, *2*, 407.
- [22] T. X. Jiang, R. B. Wideltz, W. M. Shen, P. Will, D. Y. Wu, C. M. Lin, H. S. Jung, C. M. Chuong, *Int. J. Dev. Biol.* **2004**, *48*, 117.
- [23] C. M. Chuong, C. Y. Yeh, T. X. Jiang, R. Wideltz, *Wiley Interdiscip. Rev. Dev. Biol.* **2013**, *2*, 97.
- [24] H. C. Chiu, C. H. Chang, J. S. Chen, S. H. Jee, *J. Formos. Med. Assoc.* **1996**, *95*, 667.
- [25] C. A. Higgins, G. D. Richardson, D. Ferdinando, G. E. Westgate, C. A. Jahoda, *Exp. Dermatol.* **2010**, *19*, 546.
- [26] K. Inoue, N. Aoi, Y. Yamauchi, T. Sato, H. Suga, H. Eto, H. Kato, Y. Tabata, K. Yoshimura, *J. Cell Mol. Med.* **2009**, *13*, 4643.
- [27] C. A. Jahoda, A. J. Reynolds, C. Chaponnier, J. C. Forester, G. Gabbiani, *J. Cell Sci.* **1991**, *99*(Pt 3), 627.
- [28] Y. Miao, Y. B. Sun, B. C. Liu, J. D. Jiang, Z. Q. Hu, *Tissue Eng. Part A* **2014**, *20*, 2329.
- [29] K. Yamauchi, A. Kurosaka, *Arch. Dermatol. Res.* **2009**, *301*, 357.
- [30] R. Paus, S. Muller-Rover, C. Van Der Veen, M. Maurer, S. Eichmuller, G. Ling, U. Hofmann, K. Foitzik, L. Mecklenburg, B. Handjiski, *J. Invest. Dermatol.* **1999**, *113*, 523.
- [31] L. Ahtiainen, S. Lefebvre, P. H. Lindfors, E. Renvoise, V. Shirokova, M. K. Vartiainen, I. Thesleff, M. L. Mikkola, *Dev. Cell* **2014**, *28*, 588.
- [32] T. Andl, S. T. Reddy, T. Gaddapara, S. E. Millar, *Dev. Cell* **2002**, *2*, 643.
- [33] D. L. Gay, C. C. Yang, M. V. Plikus, M. Ito, C. Rivera, E. Treffeisen, L. Doherty, M. Spata, S. E. Millar, G. Cotsarelis, *J. Invest. Dermatol.* **2015**, *135*, 45.
- [34] J. Huelsken, R. Vogel, B. Erdmann, G. Cotsarelis, W. Birchmeier, *Cell* **2001**, *105*, 533.
- [35] C. G. Schirren, W. H. Burgdorf, C. A. Sander, G. Plewig, *Am. J. Dermatopathol.* **1997**, *19*, 335.
- [36] C. M. Lin, T. X. Jiang, R. E. Baker, P. K. Maini, R. B. Wideltz, C. M. Chuong, *Dev. Biol.* **2009**, *334*, 369.
- [37] S. Kondo, *J. Theor. Biol.* **2017**, *414*, 120.
- [38] B. Ermentrout, *Proc. R. Soc. Lond. A Math. Phys. Sci.* **1991**, *434*, 413.
- [39] A. L. Krause, V. Klika, T. E. Woolley, E. A. J. P. R. E. Gaffney, *Phys. Rev. E* **2018**, *97*, 052206.
- [40] Y. Wang, H. Chang, J. Nathans, *Development* **2010**, *137*, 4091.
- [41] B. Gworys, Z. Domagala, *Ann. Anat.* **2003**, *185*, 383.
- [42] P. Sengel, A. Mauger, *Dev. Biol.* **1976**, *51*, 166.
- [43] B. St-Jacques, H. R. Dassule, I. Karavanova, V. A. Botchkarev, J. Li, P. S. Danielian, J. A. McMahon, P. M. Lewis, R. Paus, A. P. McMahon, *Curr. Biol.* **1998**, *8*, 1058.
- [44] K. Foitzik, R. Paus, T. Doetschman, G. P. Dotto, *Dev. Biol.* **1999**, *212*, 278.
- [45] J. Kishimoto, R. E. Burgeson, B. A. Morgan, *Genes Dev.* **2000**, *14*, 1181.
- [46] A. Osada, T. Iwabuchi, J. Kishimoto, T. S. Hamazaki, H. Okochi, *Tissue Eng.* **2007**, *13*, 975.
- [47] C. S. Harmon, T. D. Nevins, W. B. Bollag, *Br. J. Dermatol.* **1995**, *133*, 686.
- [48] V. A. Botchkarev, N. V. Botchkareva, A. A. Sharov, K. Funa, O. Huber, B. A. Gilchrist, *J. Invest. Dermatol.* **2002**, *118*, 3.
- [49] J. Okano, C. Levy, U. Lichti, H. W. Sun, S. H. Yuspa, Y. Sakai, M. I. Morasso, *J. Biol. Chem.* **2012**, *287*, 39304.
- [50] X. J. Zhu, Y. Liu, Z. M. Dai, X. Zhang, X. Yang, Y. Li, M. Qiu, J. Fu, W. Hsu, Y. Chen, Z. Zhang, *PLoS Genet.* **2014**, *10*, e1004687.
- [51] R. L. Thangapazham, P. Klover, S. Li, J. A. Wang, L. Sperling, T. N. Darling, *Exp. Dermatol.* **2014**, *23*, 443.
- [52] J. D. Glover, K. L. Wells, F. Matthaus, K. J. Painter, W. Ho, J. Riddell, J. A. Johansson, M. J. Ford, C. A. B. Jahoda, V. Klika, R. L. Mort, D. J. Headon, *PLoS Biol.* **2017**, *15*, e2002117.
- [53] A. E. Shyer, A. R. Rodrigues, G. G. Schroeder, E. Kassianidou, S. Kumar, R. M. Harland, *Science* **2017**, *357*, 811.
- [54] T. X. Jiang, H. S. Jung, R. B. Wideltz, C. M. Chuong, *Development* **1999**, *126*, 4997.
- [55] W. K. W. Ho, L. Freem, D. Zhao, K. J. Painter, T. E. Woolley, E. A. Gaffney, M. J. McGrew, A. Tzika, M. Milinkovitch, P. Schneider, A. Drusko, F. Matthäus, J. L. Glover, K. L. Wells, J. A. Johansson, M. G. Davey, H. M. Sang, M. Clinton, D. J. Headon, *PLoS Biol.* in press.
- [56] M. Inaba, H. I.-C. Harn, C. M. Chuong, *PLoS Biol.* in press.
- [57] Y. Soneoka, P. M. Cannon, E. E. Ramsdale, J. C. Griffiths, G. Romano, S. M. Kingsman, A. J. Kingsman, *Nucleic Acids Res.* **1995**, *23*, 628.

## SUPPORTING INFORMATION

Additional supporting information may be found online in the Supporting Information section at the end of the article.

**Figure S1.** A generic working model for planar skin reconstitution with hair formation. Epidermal and dermal cells are mixed and plated on tissue culture insert in high cell density as a droplet. Different epidermal and dermal cells can be used, those derive from newborn skin, adult skin, adult hair follicle, and ES or iPS derived cells

**Figure S2.** Live cell imaging of hair peg-like structures. A, Overexpression of fluorescent proteins did not affect the ability to form hair peg-like structures. In this image, epidermal cell nuclei were marked with green fluorescent protein and dermal cell nuclei were preferentially marked with orange fluorescent protein. The dotted line outlines the epidermal stalk. Epi = epidermal, D = dermal, E = epidermal (n = 7). B, A still image from a two-color live imaging video (Figure S5A), looking down from the top of the culture droplet, demonstrates a dermal cap. p63-positive keratinocyte nuclei are magenta, dermal cell nuclei are cyan. Epi SC = epidermal stem cell (n = 5). C, A single lateral image taken from a three-color live imaging video (Figure S5B) demonstrates a hair peg-like structure. Keratinocyte nuclei are orange, p63-positive keratinocyte nuclei are magenta, and dermal cell nuclei are cyan (n = 5)

**Figure S3.** Reconstituted hair peg-like structures displayed radial symmetry. Cap and stalk sagittal areas maintained a linear relationship with the total cap and stalk volumes, emphasizing the radial symmetry of these structures and allowing us to simplify analysis by measuring the area of each structure at the midpoint corresponding to maximal width

**Movie S1** Three-dimensional z-stack reconstructions of human hair peg-like structures formed in culture. A, Whole mount confocal z-stack images of multiple hair peg-like structures immunostained with keratin-14 (green), vimentin (red), and TO-PRO-3 iodide (nuclei, blue) demonstrate the periodic patterning and formation of distinct structures within a 425  $\mu\text{m}^2$  area. Cells within the keratinized sheet were difficult to stain with pancytokeratin due to poor antibody penetration. B, Whole mount confocal z-stack images of hair peg-like structures immunostained with pancytokeratin (green) and propidium iodide (nuclei, red) demonstrate the spherical configuration of the dermal cap and the tubular structure of the epidermal stalk. Sandwiching of the whole mount culture beneath a coverslip for confocal imaging caused the hair pegs to appear bent or flattened against the keratinocyte sheet. C, Higher magnification view of a single reconstituted human hair peg-like structure immunostained with pancytokeratin (green) and propidium iodide (nuclei, red). Note epidermal cells start to wrap around the dermal cap

**Movie S2** Three-dimensional z-stack reconstructions of reconstituted human hair peg-like structures demonstrate markers of dermal papilla gene expression. A, Whole mount confocal z-stack imaging demonstrates  $\alpha$ -SMA staining in a central location within the dermal

cap of a hair peg-like structure.  $\alpha$ -SMA (green), propidium iodide (red). B, Whole mount confocal z-stack imaging demonstrates the presence of extracellular collagen IV at the epidermal-dermal interface. CD34 - an early dermal papilla marker (green), collagen IV (red), TO-PRO-3 iodide (blue). The large green lobules are artifacts representing dead cells which have trapped the dye

**Movie S3** Three-dimensional z-stack reconstructions of epidermal placode-like structures and dermal clusters at 48 hours. A, Whole mount confocal z-stack imaging demonstrates multiple dermal clusters atop a keratinocyte sheet and altered keratinocyte arrangement pattern around the dermal clusters. Pancytokeratin (green), propidium iodide (red). The large green lobules are artifacts representing dead cells which have trapped the dye. B, Whole mount confocal z-stack imaging demonstrating vimentin-positive immunostaining of the dermal clusters at 48 hours post-plating. Vimentin (red), TO-PRO-3 iodide (blue)

**Movie S4** Live cell imaging of a reconstituted human hair peg-like structure. Time-lapse movie highlighting dermal cell shape and movement within the dermal cap of a reconstituted human hair peg-like structure, as viewed from the top of a culture droplet. The epidermal stalk is not visible in this view. A z-stack image was recorded every 10 minutes from 101-103 hours post-plating and is replayed at a rate of 5 frames per second. The entire culture descended along the z-axis during imaging, resulting in partial movement out of the focal plane over time. p63-positive epidermal cells were labelled with nuclear eGFP fluorescent protein (magenta). Dermal cells were labelled with nuclear mCerulean3 fluorescent protein (cyan). Note the varied dermal cell movement and nuclear shape within the dermal cap. Few p63-positive epidermal cells are visible in this top-down view, as the epidermal stalk is obscured by the cells of the dermal cap. However, reproducibly, 1-3 p63-positive epidermal cells were noted within the dermal cap, frequently at the apex, as seen here

**Movie S5** Live cell imaging of a reconstituted human hair peg-like structure. Time-lapse movie of a reconstituted human hair peg-like structure, viewed from top-down (A) and lateral (B) orientations. A z-stack image was recorded every 10 minutes from 83-85 hours post-plating and is replayed at a rate of 10 frames per second. All epidermal nuclei were pre-labelled with mOrange2 fluorescent protein (yellow). p63-positive epidermal nuclei were labelled with eGFP (magenta). Dermal nuclei were labelled with mCerulean3 fluorescent protein (cyan). Note that the entire specimen drifts during imaging. However, the epidermal cells within the epidermal sheet remain static, as evidenced by no change in positional relationship with adjacent epidermal cells. The position of the dermal cap does move in space, relative to the epidermal sheet, because the epidermal stalk is flexible and sways within the droplet culture medium

**Movie S6** Mathematical simulation of human hair follicle periodic pattern formation in vitro. The changes in periodic patterning from long stripes to short stripes to punctate clusters, corresponding to

dermal clusters and then hair peg-like structures, is represented here by a Turing-based mathematical simulation. The periodic patterns form sequentially on the left, as the radially symmetric spatiotemporal gradient increases in the middle and right-sided diagrams.

**Appendix S1** Supplemental Methods

**Table S1** Antibodies

**Table S2** Primers for lentiviral vector construction. gDNA = genomic DNA

**Table S3** Parameter values for equations (1)-(4)

**How to cite this article:** Weber EL, Woolley TE, Yeh C-Y, Ou K-L, Maini PK, Chuong C-M. Self-organizing hair peg-like structures from dissociated skin progenitor cells: New insights for human hair follicle organoid engineering and Turing patterning in an asymmetric morphogenetic field. *Exp Dermatol*. 2019;28:355-366. <https://doi.org/10.1111/exd.13891>